Diffusion bonding of RAFM steels: evolution of interfacial oxide layer with pressure and microstructure and mechanical property after post bonding heat treatment

J.-G. Chen [a]*, W.-J. Wang [b], J. Dong [a], C.-C. Wang [a], Y.-S. Wei [b]

[a] *School of Mechanical Engineering, Tianjin Sino-German University of Applied Sciences, Tianjin 300350, P.R. China*
[b] *Tianjin Special Equipment Inspection Institute, Tianjin 300192, P.R. China*

*Corresponding author (Jianguo Chen): e-mail address: chenjianguo@tsguas.edu.cn
Wanjun Wang: e-mail address: wanxiya1022@163.com
Ji Dong: e-mail address: dongji@tsguas.edu.cn
Chuancai Wang: e-mail address: wangchuancai@tsguas.edu.cn
Yushun Wei: e-mail address: yswei7964@163.com

(Received 11 October 2023; Accepted 13 March 2024)

Abstract

The effect of elevating the bonding pressure from 10 to 20 MPa (5 MPa interval) at 1050 ºC for 60 minutes on the diffusion bonded joint of reduced activation ferritic/martensitic (RAFM) steel was studied. The results indicate that as the bonding pressure increases, the joint quality correspondingly improves. The oxide layer at the bonding interface underwent an evolution process from continuous to discontinuous and ultimately disappeared with the increase of bonding pressure. The optimal joint was achieved at the pressure of 20 MPa in this work. Considering the exploration of joint reliability in engineering applications, the optimal joint was subjected to a post bonding heat treatment (PBHT) of 750 ºC for 90 minutes. The diffusion bonded sample subjected to PBHT displays microstructural characteristics and tensile properties similar to those of the base metal. Notably, tensile fracture does not occur at the bonding interface, but in the base metal far from the interface. This work can provide a feasible method for the removal of oxides at the diffusion bonding interface of RAFM steel, and also contribute to the establishing and optimization of diffusion bonding processes, thereby improving the quality of diffusion bonded joint.

Keywords：Bonding pressure; Oxide layer; Microstructure; Mechanical property

1. Introduction

Reduced activation ferritic/martensitic (RAFM) steel is frequently chosen as the primary material for the main structure of fusion reactor blanket module due to its impressive high-temperature mechanical attributes, superior radiation swelling resistance, low thermal expansion coefficient, and favorable processing performance [1-3]. Reliable welding methodology for RAFM steel is the key to manufacturing blanket module. The fusion welding involves the melting of the base metal to create a molten pool, which then solidifies through a non-equilibrium process. Thus, fusion welding techniques such as laser beam or arc welding or even solid-state friction stir welding may result in the formation of undesirable brittle phases in structural steels [4-6]. In addition to the undesirable variations in the microstructure and mechanical

properties, fusion welding also lead to a concentration of residual stress in the welded joint, which often becomes the weakest link of components. More importantly, a large number of researches show that long-term creep in fusion welded joints of high Cr ferritic/martensitic steel leads to inevitable type IV fracture failure, resulting in the creep life of joints much lower than that of base metal [7-9]. The fact that the blanket module is continuously subjected to high-temperature and high-radiation conditions only further deteriorates the strength of the joint. Therefore, the solid phase welding technology represented by diffusion bonding is expected to make up for the shortcomings of fusion welding and become a potential alternatives to fusion welding for the assembly of RAFM steel components, due to its outstanding advantages such as low welding temperature, small welding deformation, and high dimensional assembly accuracy.

Diffusion bonding is a solid bonding process that applies pressure to two or more solid phase materials at high-temperature to cause microscopic plastic deformation at the bonding interface, and maintains a period of time to form a solid metallurgical bond through atomic diffusion [10]. The key elements influencing diffusion bonding include temperature, pressure, and time. So far, some research has been conducted on the diffusion bonding of RAFM steel [11-13]. However, most of these studies have primarily focused on the variables of bonding temperature and bonding time, with limited attention given to the bonding pressure. This article intends to explore the role of bonding pressure in the diffusion bonding of RAFM steel. Additionally, considering the practical engineering applications, the joint with the best bonding quality in this study was subjected to post bonding heat treatment (PBHT), and its mechanical properties were assessed.

2. Materials and experiment methods

2.1 Diffusion bonding experiment

The RAFM steel was cast in a vacuum induction furnace into an ingot weight 25 kg, then forged into cylinder bars with a size of 350 mm in height and 120 mm in diameter. The chemical composition of the experimental steel can be found in Table 1. The initial RAFM steel base sample was normalized at 1050 ^{o}C for 30 minutes and tempered at 750 ^{o}C for 90 minutes. Its microstructure reveals tempered martensite with a small amount of δ-ferrite, as depicted in Fig. 1. The substrate used for processing the diffusion bonded sample was cut out from the steel sample and uniformly polished, resulting in a disc with 60 mm diameter and 10 mm height. Then, cylindrical sample blocks with a diameter and height of 10 mm were cut from the disc. The blocks were paired up to conduct diffusion bonding test using the Gleeble-3500 thermal simulator. Prior to diffusion bonding, the sample blocks were ultrasonically cleaned in acetone and alcohol, and then dried. The sample blocks to be bonded were heated to 1050 ^{o}C at a heating rate of 100 ^{o}C/min, and maintained under various pressure namely 10, 15, and 20 MPa for 60 minutes. After that the pressure was relieved, then the bonded specimen was cooled to room temperature. The vacuum level during diffusion bonding was maintained at 1×10^{-4} Pa.

Table 1

C	Cr	W	Mn	Si	V	Ta	Fe

0.08	8.93	1.54	0.53	0.05	0.29	0.12	Bal.

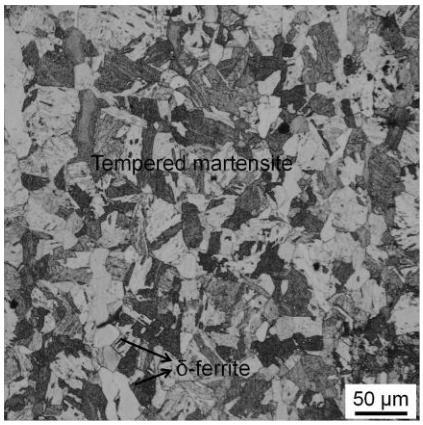

Figure 1

2.2. Microstructure observation and tensile property

The examination of the microstructure at diffusion bonding interface was carried out with a Zeiss Gemini SEM500 scanning electron microscope (SEM). Following grinding and mechanical polishing, the samples were treated with an etching solution composed of 20 mL hydrochloric acid, 100 mL water and 5g ferric chloride. The evolution of oxides at the diffusion bonding interface under varying bonding pressures was studied using an energy dispersive spectroscopy (EDS). The precipitates of diffusion bonded sample after PBHT were identified using a Jem-2100f transmission electron microscopy (TEM). For testing the tensile attributes of the diffusion bonding sample, a specimen with a 4 mm gauge length was employed. The bonding interface was located in the middle of the tensile specimen. The tensile properties were evaluated at room-temperature on an Instron 8871 using a strain rate of 1×10^{-3} s^{-1}.

3. Results and discussion

3.1. Microstructure of the diffusion bonded samples

3.1.1. SEM observation

Fig. 2 presents the SEM images of the diffusion bonding interface obtained at 1050 ^{o}C for 60 minutes upon pressures of 10, 15, and 20 MPa, respectively. The bonding interface is indicated by the black arrow in the figure. It can be observed that there are no remarkable microstructure differences or gradients in close proximity to the bonding interface. Due to the fact that this work involves the direct diffusion bonding of metal solid, there is an absence of a transition layer at the bonding interface. The bonding interface of joint obtained at 10 MPa is easily identifiable, implying that the joint has not yet achieved complete metallurgical bonding. As the bonding pressure intensifies, the interface gradually becomes blurry. When the bonding pressure is 15 MPa, some grains on both sides of the bonding interface grow reciprocally and traverse the bonding interface. The mutual growth and fusion of grains on both sides of the bonding interface into new grains represents a good development trend in bonding quality [14]. The bonding pressure is further increased to 20 MPa, the bonding interface is difficult to distinguish, and the microstructure on either side of the bonding interface is fully continuous. It can be concluded that

increasing the bonding pressure from 10 to 20 MPa significantly enhances the quality of the diffusion bonded joint.

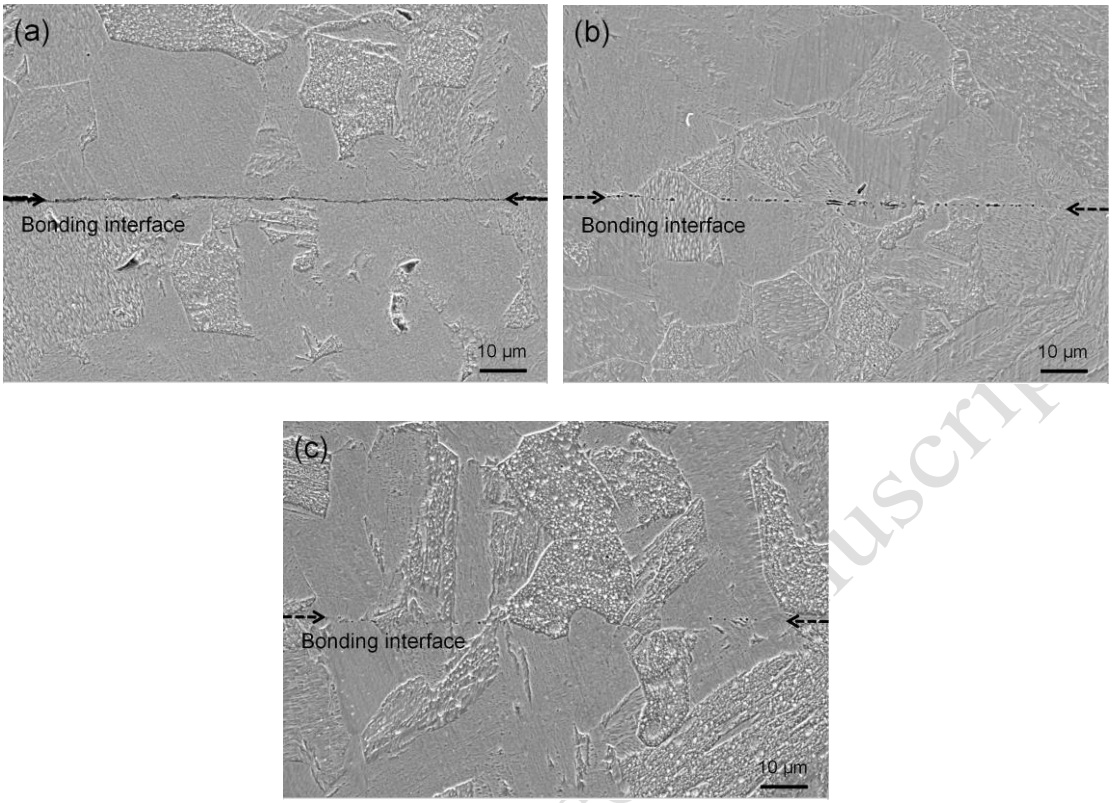

Figure 2

3.1.2. EDS analysis

Fig. 3 shows the EDS mapping analysis of the diffusion bonding interface obtained at 1050 ^{o}C for 60 minutes upon pressures of 10, 15, and 20 MPa, respectively. It reveals a high concentration of Chromium (Cr), Oxygen (O) and manganese (Mn), and a low concentration of Iron (Fe) around the bonding interface at a pressure of 10 MPa, and the distribution of Cr/Mn rich oxide is continuous, as displayed in Fig. 3(a). The thickness of the oxide layer is approximately 0.65 μm. It should be pointed out that the Cr content in RAFM steel is relatively high. Despite meticulous sanding and polishing were carried out during the preparation process of the samples to be bonded, even short exposure of the machined surface allows Cr to easily react with O, forming Cr rich oxides [15]. Meanwhile, the Mn content is also higher at the interface of 10 MPa and 15 MPa, as Mn is also easily bound to O. There is no significant difference in tungsten (W) concentration at the interface. As the bonding pressure escalates from 15 to 20 MPa, the concentration fluctuations of Cr, Mn, Fe and O at the interface disappear, and the oxide gradually becomes sporadic until it entirely vanishes, as illustrated in Figs. 3(a) and 3(c). This occurs because a higher bonding pressure augments the probability of plastic deformation of micro protrusions on the bonding surface, thereby increasing the close contact area at the bonding interface and leading to the rupture of the oxide layer. Moreover, Sharma et al. [16] confirmed that plastic deformation at the interface caused by pressure can bolster the plastic flow of the material at the bonding interface and facilitate the

rupture of the oxide layer. The rupture of high-level oxide layer caused by high bonding pressure effectively heightens the direct contact of exposed metals, providing sufficient diffusion channels for atomic diffusion, which is more favorable for achieving mutual diffusion between atoms [17]. Simultaneously, the plastic deformation at the bonding interface places the atoms at that location to be in a state of high deformation energy, making them easier to diffuse [18]. In addition, EDS analysis also validates that as the bonding pressure increases from 10 to 20 MPa, the element distribution at the bonding interface is becoming increasingly uniform, and there is no fluctuation in element content. This further corroborates the adequacy of element diffusion at the interface. It should be emphasized that while bonding pressure can improve the quality of joints, excessive bonding pressure can cause deformation or even cracking of the workpiece, which is not beneficial for manufacturing structural components. The selection of bonding pressure should balance meeting engineering application requirements and preventing deformation of the welded parts.

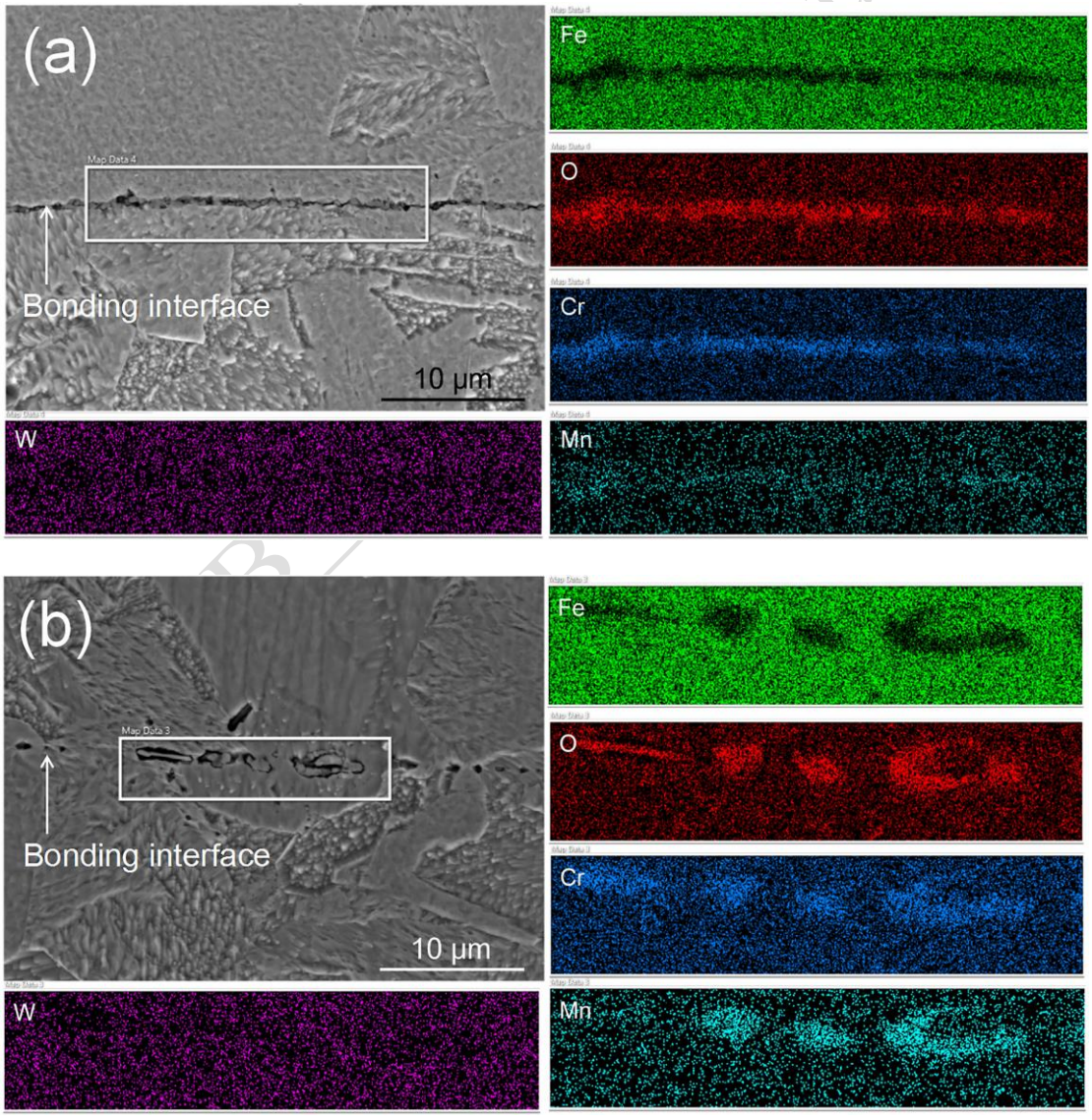

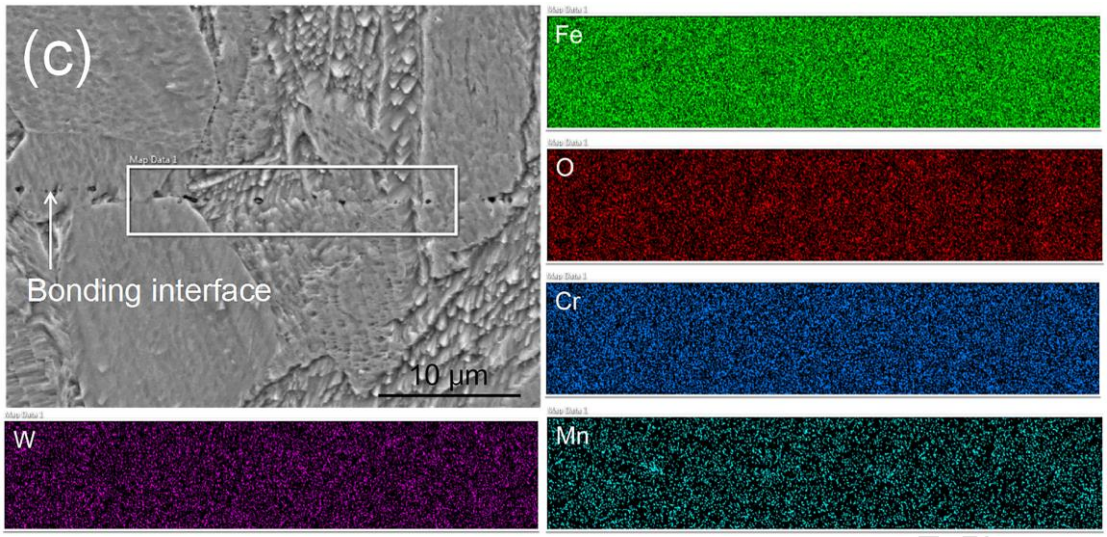

Figure 3

3.1.3. SEM and TEM observations of the diffusion bonded sample subjected to PBHT

It is found that the bonding quality of the diffusion bonding sample produced at 1050 ºC for 60 minutes upon the pressure of 20 MPa is the best in this study through prior analysis of the diffusion bonding process. Thus, the diffusion bonded joint obtained at 20 MPa is selected as the subsequent research object. Given the requirements of engineering applications, the joint is subjected to a PBHT of 750 ºC tempering for 90 minutes. Fig. 4 shows the SEM and TEM images of the diffusion bonding sample after PBHT. SEM detection reveals a significant amount of precipitates in the microstructure, while the bonding interface remains indistinct. The precipitates near the diffusion bonding interface were extracted by means of carbon extraction replica technique and examined by TEM. It was found that the precipitates are primarily located at the prior austenite grain boundary (green schematic line diagonally downwards to the right) and martensite lath boundary (yellow schematic line diagonally upward to the right), as illustrated in Fig. 4(b). The type of precipitate is determined as $M_{23}C_6$-type carbides by electron diffraction pattern analysis. This is similar to the precipitation strengthening method of RAFM steel without diffusion bonding after tempering treatment in previous studies, that is, $M_{23}C_6$-type carbides are precipitated at the prior austenite grain boundary and martensite lath boundary to achieve precipitation strengthening [19,20]. The above analysis indicates that there is no significant difference in microstructure and precipitation strengthening method between RAFM steel with direct diffusion bonding followed by PBHT and the base metal without bonding after tempering treatment.

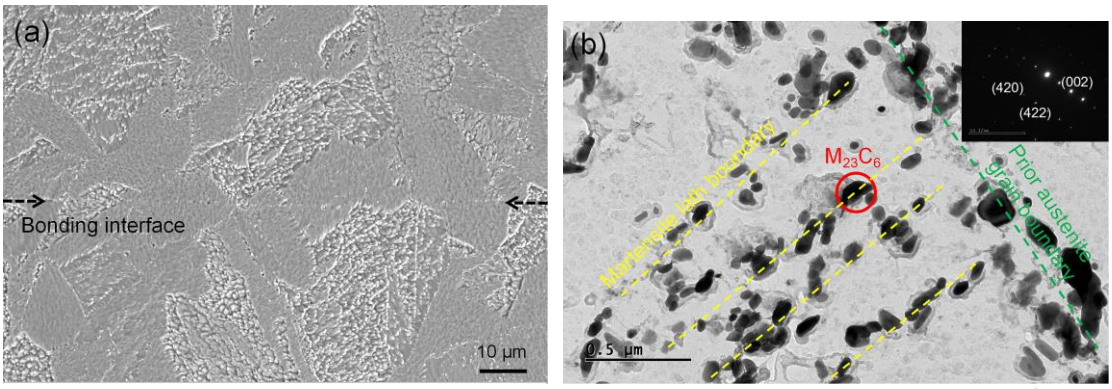

Figure 4

3.2. Mechanical property of the diffusion bonded sample

The tensile properties of the optimal bonded RAFM steel (obtained at 20 MPa) were tested before PBHT, with a tensile strength of 950 MPa and an elongation of 8.5%. The plasticity is too poor. Moreover, the final service state of RAFM steel is a high-temperature tempered state, which can ensure the precipitation of a large amount of precipitates in the matrix to meet all performance requirements [21]. Therefore, PBHT of the diffusion bonded joint is necessary. Fig. 5 presents the comparison between the tensile properties of the diffusion bonded sample after PBHT with the original normalized and tempered base sample. It can be found that the tensile strength and total elongation of the diffusion bonded sample are comparable to those of the original base metal sample, with a tensile strength around 680 MPa and a total elongation of approximately 22%. Observing the diffusion bonding sample after fracture, it is evident that the fracture position is located on the base metal far from the bonding interface, as shown in the tensile fracture pattern in the upper right corner of Fig. 5. This can be explained by the fact that the plastic deformation caused by micro protrusions at the bonding interface during diffusion bonding is relatively higher than that of the base material, which leads to a higher dislocation density at the interface, and more subgrain boundaries are formed to precipitate more carbides during PBHT, thus resulting in higher strength at the bonding interface [22]. SEM examination on the tensile fracture of the diffusion bonded sample is performed, as demonstrated in Fig. 6. Significant necking can be observed in the tensile fracture observed at low magnification, accompanied by obvious shear lips at the outer periphery, as shown in Fig. 6(a). High magnification observation of tensile fracture surface in Fig. 6(b) reveals the presence of conspicuous dimples with various sizes in the fracture, indicating that the fracture mechanism is ductile fracture.

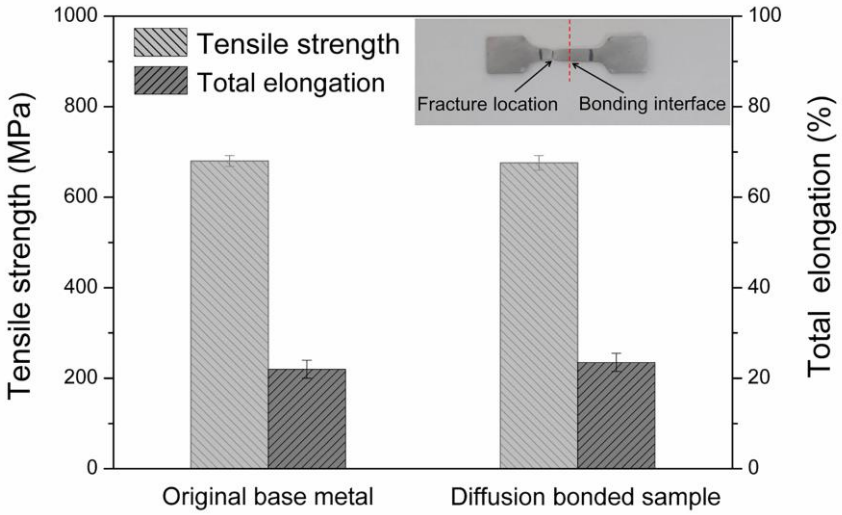

Figure 5

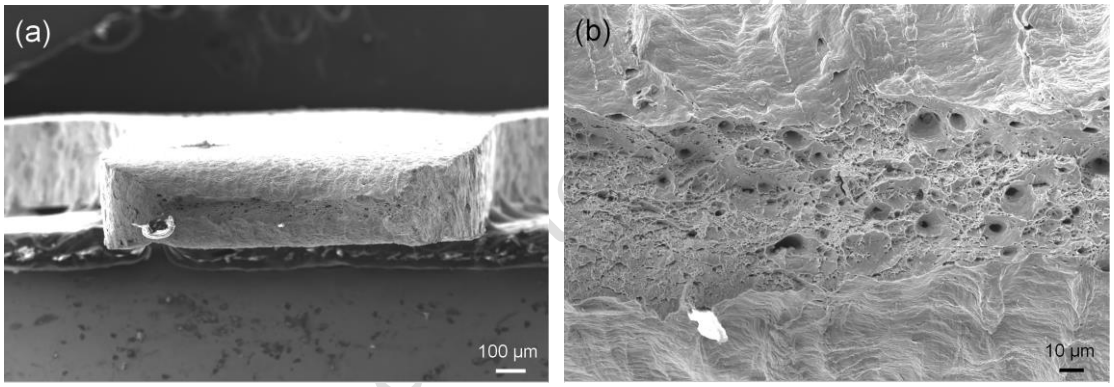

Figure 6

Based on the above analysis, it can be preliminarily considered that the diffusion bonding of RAFM steel can satisfies the requirements of engineering applications. This can be explained by the following two reasons. On the one hand, the microstructure and element transition of the prepared bonding joint are uniform, and there is no formation of non-equilibrium microstructure. On the other hand, the strength and plasticity of the bonding joint are not lower than those of the base metal.

4 Conclusions

This work investigated the influence of bonding pressure on the RAFM steel diffusion bonded joints, and the microstructure and mechanical property of the optimal joint subjected to PBHT. The main results are as follows:

(1) The quality of the diffusion bonded joints held at 1050 ^{o}C for 60 minutes gradually improves as the bonding pressure increases from 10 to 20 MPa. The specific manifestation is that the oxides at the bonding interface evolves from continuous distribution to discontinuous distribution, and ultimately disappears completely.

(2) After PBHT, the tensile properties of the diffusion bonded joint obtained at 1050 ^{o}C for 60 minutes with a pressure of 20 MPa are comparable to those of the base

metal.

(3) The tensile fracture of the diffusion bonded specimen is located at the base metal far from the bonding interface.

Acknowledgements

This work was financially supported by the Science&Technology Development Fund of Tianjin Education Commission for Higher Education (No. 2023KJ250).

Authorship contributions

Jianguo Chen: Experimental scheme and design, Paper writing, Supervision. Wanjun Wang: Investigation. Ji Dong: Translation and revision. Chuancai Wang: Investigation. Yushun Wei: Formal analysis.

Data availability

All data generated or analyzed during this work are included in this published article.

Conflicts of interests

The authors declare that they have no known competing financial interests that could have appeared to influence the work reported in this paper.

References

[1] X.S. Zhou, C.X. Liu, L.M. Yu, Y.C. Liu, H.J. Li, Phase transformation behavior and microstructural control of high Cr martensitic/ferritic heat-resistant steels for power and nuclear plants: a review, Journal of Materials Science & Technology, 31 (2015) 235-242. https://doi.org/10.1016/j.jmst.2014.12.001

[2] K.C. Sahoo, K. Laha, Influence of thermal ageing on tensile-plastic flow and work hardening parameters of Indian reduced activated ferritic martensitic steel, Journal of Mining and Metallurgy, Section B: Metallurgy, 59 (2023) 217-229. https://doi.org/10.2298/JMMB221114019S

[3] J.G. Chen, C.X. Liu, C. Wei, Y.C. Liu, H.J. Li, Effects of isothermal aging on microstructure and mechanical property of low-carbon RAFM steel, Acta Metallurgica Sinica (English Letters), 32 (2019) 1151-1160. https://doi.org/10.1007/s40195-019-00883-6

[4] G. Cam, S. Erim, C. Yeni, M. Kocak, Determination of mechanical and fracture properties of laser beam welded steel joints, Welding Journal, 78 (6) (1999) 193s-201s.

[5] G. Cam, M. Kocak, J.F. dos Santos, Developments in laser welding of metallic materials and characterization of the joints, Welding in the World, 43 (2) (1999) 13-26.

[6] U. Gürol, B. Turgut, H. Kümek, S. Dilibal, M. Koçak, Fabrication and characterization of wire arc additively manufactured ferritic-austenitic bimetallic structure, Metals and Materials International, (2023). https://doi.org/10.1007/s12540-023-01568-7

[7] J.A. Francis, W. Mazur, H.K.D.H. Bhadeshia, Type IV cracking in ferritic power plant steels, Materials Science and Technology, 22 (2006) 1387-1395. https://doi.org/10.1179/174328406X148778

[8] H. Hongo, M. Tabuchi, T. Watanabe, Type IV creep damage behavior in Gr.91 steel welded joints, Metallurgical and Materials Transactions A, 43 (2011) 1163-1173. https://doi.org/10.1007/s11661-011-0967-6

[9] D.J. Abson, J.S. Rothwell, Review of type IV cracking of weldments in 9-12%Cr creep strength enhanced ferritic steels, International Materials Reviews, 58 (2013) 437-473.

https://doi.org/ 10.1179/1743280412Y.0000000016

[10] C. Wei, Z. Wang, X. Wang, Y. Guo, J.G. Chen, Fabrication and assessment of China low activation martensitic (CLAM) steels solid diffusion bonded joint, Fusion Engineering and Design, 174 (2022) 112987.
https://doi.org/10.1016/j.fusengdes.2021.112987

[11] C. Li, Q. Huang, Q. Wu, S. Liu, Y. Lei, T. Muroga, T. Nagasaka, J. Zhang, J. Li, Welding techniques development of CLAM steel for Test Blanket Module, Fusion Engineering and Design, 84 (2009) 1184-1187.
https://doi:10.1016/j.fusengdes.2008.12.039

[12] J.G. Chen, C.X. Liu, C. Wei, Y.C. Liu, H.J. Li, Study on microstructure and mechanical properties of direct diffusion bonded low-carbon RAFM steels, Journal of Manufacturing Processes, 43 (2019) 192-199.
https://doi.org/10.1016/j.jmapro.2019.05.020

[13] H.Y. Fu, T. Nagasaka, T. Muroga, A. Kimura, J.M. Chen, Microstructural characterization of a diffusion-bonded joint for 9CrODS and JLF-1 reduced activation ferritic/martensitic steels, Fusion Engineering and Design, 89 (2014) 1658-1663.
https://doi.org/10.1016/j.fusengdes.2014.02.055

[14] X.P. Ren, X.H. Chen, Z.P. Xiong, Characterization and analysis of diffusion bonding process in a Cr25Ni7Mo4MnSi duplex stainless steels, Journal of Manufacturing Processes, 34 (2018) 603-613.
https://doi.org/10.1016/j.jmapro.2018.07.005

[15] Y. Zhao, C. Li, B. Huang, S. Liu, Q. Huang, FDS Team, Verification of the effect of surface preparation on Hot Isostatic Pressing diffusion bonding joints of CLAM steel, Journal of Nuclear Materials, 455 (2014) 486-490.
http://dx.doi.org/10.1016/j.jnucmat.2014.08.004

[16] G. Sharma, D.K. Dwivedi, Effect of pressure pulsation on bond interface characteristics of 409 ferritic stainless steel diffusion bonds, Vaccum, 146 (2017) 152-158.
https://doi.org/10.1016/j.vacuum. 2017.09.049

[17] K Xue, W. Tian, S. Yan, H. Li, P. Li, Variations in mechanical properties of RAFM steel under vacuum diffusion welding with pre-deformation and subsequent heat treatment, Fusion Engineering and Design, 152 (2020) 111470.
https://doi.org/10.1016/j.fusengdes.2020.111470

[18] L. Zhou, S. Feng, M. Sun, B. Xu, D. Li, Interfacial microstructure evolution and bonding mechanisms of 14YWT alloys produced by hot compression bonding, Journal of Materials Science & Technology, 35 (2019) 1671-1680.
https://doi.org/10.1016/j.jmst.2019.04.005

[19] J.G. Chen, Y.C. Liu, Y.T. Xiao, Y.H. Liu, C.X. Liu, H.J. Li, Improvement of high-temperature mechanical properties of low-carbon RAFM steel by MX precipitates, Acta Metallurgica Sinica (English Letters), 31 (2018) 706-712.
https://doi.org/10.1007/s40195-018-0703-y

[20] J.G. Chen, C.X. Liu, Y.C. Liu, B.Y. Yan, H.J. Li, Effects of tantalum content on the microstructure and mechanical properties of low-carbon RAFM steel, Journal of Nuclear Materials, 479 (2016) 295-301.
https://doi.org/10.1016/j.jnucmat.2016.07.029

[21] R.L. Klueh, Elevated temperature ferritic and martensitic steels and their application to future nuclear reactors, International Materials Reviews, 50 (2005) 287-310. https://doi.org/10.1179/174328005X41140

[22] Y. Hua, J. Chen, L. Yu, Y. Si, C. Liu, H. Li, Y. Liu, Microstructure evolution and mechanical properties of dissimilar material diffusion-bonded joint for high Cr ferrite heat-resistant steel and austenitic heat-resistant steel, Acta Metallurgica Sinica, 58 (2022) 141-154. https://doi.org/ 10.11900/0412.1961.2020.00446

Table captions:

Table 1. Chemical composition of the steel (in wt.%)

List of figure captions:

Fig.1 OM image of the original microstructure of RAFM steel

Fig.2 SEM images of RAFM steel diffusion bonded joints held at 1050 ^{o}C for 60 minutes upon different pressures: (a) 10 MPa, (b) 15 MPa, (c) 20 MPa

Fig.3 EDS mapping analyses of RAFM steel diffusion bonded joints held at 1050 ^{o}C for 60 minutes upon different pressures: (a) 10 MPa, (b) 15 MPa, (c) 20 MPa

Fig.4 SEM and TEM images of RAFM steel diffusion bonded joint held at 1050 ^{o}C for 60 minutes upon 20 MPa subjected to PBHT

Fig.5 Comparison of tensile property for original base metal and diffusion bonded joint (prepared at 1050 ^{o}C for 60 minutes upon 20 MPa) subjected to PBHT

Fig.6 SEM images at low (a) and high (b) magnification of tensile fracture of RAFM steel diffusion bonded joint held at 1050 ^{o}C for 60 minutes upon 20 MPa subjected to PBHT